

Investigation of Heat Conductivity in Relativistic Systems using a Partonic Cascade

M. Greif,^{1,*} F. Reining,¹ I. Bouras,¹ G. S. Denicol,² Z. Xu,³ and C. Greiner¹

¹*Institut für Theoretische Physik, Johann Wolfgang Goethe-Universität,
Max-von-Laue-Str. 1, D-60438 Frankfurt am Main, Germany*

²*Department of Physics, McGill University, 3600 University Street, Montreal, Quebec H3A 2T8, Canada*

³*Department of Physics, Tsinghua University, Beijing 100084, China*

(Dated: February 24, 2022)

Motivated by the classical picture of heat flow we construct a stationary temperature gradient in a relativistic microscopic transport model. Employing the relativistic Navier-Stokes ansatz we extract the heat conductivity κ for a massless Boltzmann gas using only binary collisions with isotropic cross sections. We compare the numerical results to analytical expressions from different theories and discuss the final results. The directly extracted value for the heat conductivity can be referred to as a literature reference within the numerical uncertainties.

I. INTRODUCTION

Ultrarelativistic heavy ion collisions (HIC) at the Relativistic Heavy Ion Collider (RHIC) and the Large Hadron Collider (LHC) create a hot and dense system of strongly interacting nuclear matter that only existed in nature a few microseconds after the Big Bang [1–3]. At such energies, quarks and gluons are deconfined and a new state of matter is formed, the Quark-Gluon Plasma (QGP). The main experimental discovery made at RHIC and LHC is that this novel state of matter behaves as a strongly coupled plasma, with the smallest viscosity to entropy density ratio, η/s , ever observed [4–7]. Currently, relativistic dissipative fluid dynamics is the main theory employed to describe the space-time evolution of the QGP formed in HIC.

The inclusion of dissipative effects in the description of the QGP started only a few years ago. To date the majority of studies have focused on investigating the effects of the shear viscosity in the time evolution of the QGP and in extracting its magnitude from HIC measurements [8–21]. Nevertheless, there are other sources of dissipation that might play a role in the fluid-dynamical description of HIC, such as bulk viscous pressure and heat flow. While bulk viscous pressure effects have already been subject to some amount of investigation [22–32], the effects of heat flow have been largely ignored.

The main reason for neglecting heat flow is that most fluid-dynamical calculations in the field attempt to describe the QGP only at midrapidity and very high energies, where baryon number and its corresponding chemical potential are approximately zero. However, when trying to describe the QGP at forward rapidities or at smaller collision energies, such as the ones probed in the RHIC low energy scan, baryon number can no longer be ignored and heat conduction or baryon number diffusion might play a more decisive role. On the other hand, before implementing heat flow in heavy ion collision simulations, it is useful to study it with more detail in simpler

systems and check how well we are able to describe it in such cases. Such types of studies were already started in Ref.[33].

In order to describe heat flow, one must know at least the heat conductivity coefficient. Currently, this is not known with the desired precision even for relativistic dilute gases. As a matter of fact, there are several expressions in the literature for this transport coefficient, e.g. from Israel-Stewart theory [34], resummed transient relativistic fluid dynamics [35], or Chapman-Enskog theory [36]. All of these methods give slightly different results and it is useful to know which one agrees best with the underlying microscopic theory in the dilute gas limit. Recently, this task has been accomplished for the case of the shear viscosity coefficient [37, 38].

In this work, we investigate the heat flow of a stationary relativistic dilute gas. Our main purpose is to obtain a precise expression for the heat conduction coefficient in the kinetic regime. In Ref. [38], this was done by imposing a stationary velocity gradient as a boundary condition, and then waiting long enough for the system to achieve the Navier-Stokes limit. Once the Navier-Stokes limit was obtained, the shear viscosity coefficient was accurately extracted as the proportionality coefficient relating the shear-stress tensor to the shear tensor. Here, we apply the method used in Ref. [38], referred to as stationary gradients method, to extract the heat conductivity of a dilute gas described by the relativistic Boltzmann equation. We solve the relativistic Boltzmann equation numerically using the transport model BAMPS (Boltzmann Approach for Multi-parton Scatterings) described in Refs. [39]. For the sake of simplicity, we shall restrict our calculations to a classical gas of massless particles, considering only elastic binary collisions with a constant isotropic cross-section.

The paper is organized as follows: In Sec. II we introduce the basic definitions of relativistic hydrodynamics. In the following Sec. III we give an overview of stationary gradients. The numerical transport model BAMPS we use in this work is introduced in Sec. IV. Next in Sec. V we derive an analytical expression for the shape of the gradients. In Sec. VI we show the method to extract the heat conductivity using BAMPS. The results obtained

* greif@th.physik.uni-frankfurt.de

from the numerical calculations are shown in Sec. VII, where we also discuss the comparison to the analytical values. Finally, we give our conclusions in Sec. VIII

Our units are $\hbar = c = k = 1$; the space-time metric is given by $g^{\mu\nu} = \text{diag}(1, -1, -1, -1)$.

II. BASIC DEFINITIONS

In relativistic kinetic theory a dilute gas of particles is characterized by the invariant particle distribution function $f(x, p)$. The macroscopic quantities are obtained from the moments of this distribution function. The first two moments of $f(x, p)$ correspond to currents of conserved quantities: the first moment of $f(x, p)$ leads to the particle four-flow (here we consider only binary collisions and, therefore, particle number is conserved),

$$N^\mu = \int \frac{g d^3 p}{(2\pi)^3 E} p^\mu f(p, x), \quad (1)$$

while the second moment corresponds to the energy-momentum tensor,

$$T^{\mu\nu} = \int \frac{g d^3 p}{(2\pi)^3 E} p^\mu p^\nu f(p, x). \quad (2)$$

Above g is the degeneracy factor, and $p^\mu = (E, \vec{p})$ is the four-momentum of the particle. Since we consider the massless limit, $E = |\vec{p}|$.

The particle four-flow and energy-momentum tensor can be decomposed with respect to an arbitrary normalized time-like four-vector, $u^\mu = \gamma(1, \vec{v})$, where $u^\mu u_\mu = 1$. The most general decomposition [36] reads

$$N^\mu = n u^\mu + V^\mu, \quad (3)$$

$$T^{\mu\nu} = \epsilon u^\mu u^\nu - P \Delta^{\mu\nu} + W^\mu u^\nu + W^\nu u^\mu + \pi^{\mu\nu}, \quad (4)$$

where $\Delta^{\mu\nu} = g^{\mu\nu} - u^\mu u^\nu$ is a projection operator onto the 3-space orthogonal to u^μ , V^μ is the particle diffusion four-current, W^μ is the energy diffusion four-current, and $\pi^{\mu\nu}$ is the shear-stress tensor. Since we are considering massless particles, the bulk viscous pressure is zero and was omitted from the decomposition above. Furthermore, we introduced the local rest frame (LRF) particle number density

$$n \equiv N^\mu u_\mu, \quad (5)$$

the LRF energy density

$$\epsilon \equiv u_\mu T^{\mu\nu} u_\nu, \quad (6)$$

and the isotropic pressure

$$P = -\Delta_{\mu\nu} T^{\mu\nu} / 3. \quad (7)$$

Notice that the particle diffusion four-current can be written in terms of N^μ as

$$V^\mu = \Delta_\nu^\mu N^\nu, \quad (8)$$

while the energy diffusion 4-current can be expressed in terms of $T^{\mu\nu}$ as,

$$W^\mu = \Delta^{\mu\alpha} T_{\alpha\beta} u^\beta. \quad (9)$$

The heat flow q^μ is defined as the difference between energy diffusion and enthalpy diffusion. For the system we are considering, it reads

$$q^\mu = W^\mu - h V^\mu, \quad (10)$$

where $h = (\epsilon + P)/n$ is the enthalpy per particle.

Without loss of generality, we use Eckart's definition of the four-velocity [40],

$$u^\mu \equiv \frac{N^\mu}{\sqrt{N^\mu N_\mu}}. \quad (11)$$

By construction, the Eckart definition of the velocity field makes the particle diffusion current vanish, $V^\mu = 0$, and, consequently, the heat flow in the Eckart frame is exactly given by the energy diffusion, i.e.,

$$q^\mu = W^\mu. \quad (12)$$

We remark that the definition of the velocity field will not affect the value of the heat conduction coefficient.

For a gas of classical particles, the thermodynamic pressure and particle number density are connected to the temperature, T , as follows,

$$p = nT. \quad (13)$$

Since we consider a massless Boltzmann gas, the thermodynamic pressure p is equal to the isotropic pressure P . The fugacity, $\lambda \equiv \exp(\mu/T)$, is given by

$$\lambda = \frac{n}{n_{\text{eq}}}, \quad (14)$$

where $n_{\text{eq}} = gT^3/\pi^2$ is the equilibrium particle number density with vanishing chemical potential.

III. STATIONARY TEMPERATURE GRADIENTS

In Navier-Stokes theory [36] heat flow is proportional to the gradient of the thermal potential, $\alpha = \mu/T$,

$$\begin{aligned} q^\mu &= -\kappa \frac{nT^2}{\epsilon + p} \nabla^\mu \alpha \\ &= \kappa \left(\nabla^\mu T - \frac{T}{\epsilon + p} \nabla^\mu p \right), \end{aligned} \quad (15)$$

where κ is defined as the heat conduction coefficient, ∂_μ is the ordinary four-derivative, $D = u^\mu \partial_\mu$ is the comoving derivative, and $\nabla^\mu \equiv \Delta^{\mu\nu} \partial_\nu = \partial^\mu - u^\mu D$ is the space-like four-gradient. For the sake of simplicity, we assume the system to be homogeneous in the y and z

plane (here referred to as the transverse direction) and resolve only the dynamics in the x -direction. We also wait long enough so that the system achieves a stationary solution, i.e., $\partial_t = 0$. In such stationary limit and with the spatial symmetries described above, the four-derivative simplifies to $\partial_\mu = (0, \partial_x, 0, 0)$.

In the stationary limit, conservation of momentum dictates that the pressure gradient must vanish. Furthermore, for small velocities, $u^x \ll 1$, the operator ∇^μ reduces to

$$\nabla^\mu = \begin{pmatrix} u_0 u_x \partial_x \\ -\partial_x \\ 0 \\ 0 \end{pmatrix}. \quad (16)$$

Then the x -component of the heat flow can be cast in the following simple form

$$q^x = \kappa (\nabla^x T) = -\kappa \partial_x T(x). \quad (17)$$

In this simplified scenario, the heat conduction coefficient can be extracted as the proportionality coefficient between the heat flow and the gradient of temperature.

IV. THE PARTONIC CASCADE BAMPS

In this work, the relativistic Boltzmann equation is solved numerically using the BAMPS simulation, developed and previously employed in Refs. [38, 39, 41–44]. This partonic cascade solves the Boltzmann equation,

$$p^\mu \partial_\mu f(x, p) = C[f], \quad (18)$$

for on-shell particles using the stochastic interpretation of transition rates. In this study we consider only binary collisions with constant isotropic cross sections. In order to reduce statistical fluctuations in simulations and to ensure an accurate solution of the Boltzmann equation (18) a testparticle method [39] is introduced: The particle number is artificially increased by multiplying it by the number of testparticles per real particle, N_{test} . The physical results are not affected by this step.

The simulation of the relativistic Boltzmann equation is performed in a static box. The transverse plane (y - z plane) of the system is assumed to be homogeneous. This is maintained by realizing the collisions of particles against the boundaries of the static box as elastic collisions off a wall. In the x -direction the boundaries of the box are fixed to have a constant gradient in temperature. In practice, this is implemented in BAMPS by removing the particles colliding with the wall in the x -direction. Independent of the absorption, the reservoirs emit particles with fixed temperature and chemical potential. The reservoirs in the left and right boundaries of the box in the x -direction, as sketched in Fig 1, are defined to have fixed temperatures, T_L^{res} and T_R^{res} , and fixed fugacities, λ_L^{res} and λ_R^{res} , respectively. Their values in our calculations are chosen to $T_L^{\text{res}} = 0.5 \text{ GeV}$, $T_R^{\text{res}} = 0.3 \text{ GeV}$. In

order to maintain no pressure gradient, we set the fugacities to $\lambda_L^{\text{res}} = 1.0$, and $\lambda_R^{\text{res}} = 7.72$. The chosen values in the reservoirs imply that, $p_L^{\text{res}} = p_R^{\text{res}} = 13.25 \text{ GeV/fm}^3$. The collective velocity in both reservoirs is set to zero.

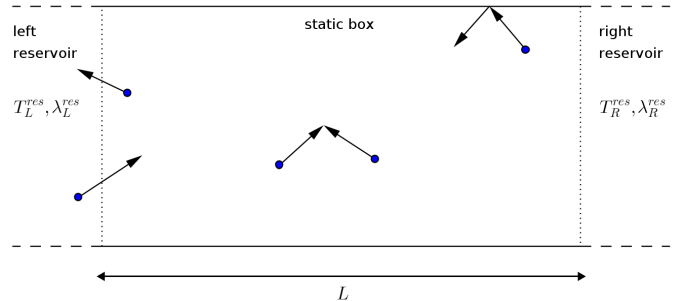


Figure 1. A sketch of the setup in BAMPS. In the left and right sides (x -direction) of the static box we introduce thermal reservoirs with fixed chemical potential and temperature.

The set of boundary conditions will lead to a stationary temperature gradient in the x -direction. Then the heat conduction coefficient can be extracted using Eq. (17). The required time for the system to reach its stationary state depends on value of the cross section, the temperature and chemical potential of the thermal reservoirs, and the initial state of the system.

Similar to the work in [38], the time the profile needs to reach the stationary profile is proportional to the inverse mean free path. This implies that the more diffuse the system is, the faster it reaches the final stationary profile and vice versa. In order to save computational time, we always initialize the system as close as possible to its stationary state.

The first step in computing the heat flow is extracting the components of the particle four-flow N^μ and energy-momentum tensor $T^{\mu\nu}$. Space in BAMPS is discretized in small volume elements, V_c . The distribution function $f(x, p)$ of this volume element is reconstructed from the momenta distribution of the particles inside it. In this scheme, the N^μ and $T^{\mu\nu}$ are computed via the discrete summation over all particles within the specific volume element and divided by the testparticle number:

$$N^\mu(t, x) = \frac{1}{V_c N_{\text{test}}} \sum_{i=1}^{N_c} \frac{p_i^\mu}{p_i^0}, \quad (19)$$

$$T^{\mu\nu}(t, x) = \frac{1}{V_c N_{\text{test}}} \sum_{i=1}^{N_c} \frac{p_i^\mu p_i^\nu}{p_i^0}, \quad (20)$$

where N_c is the total number of particles inside the corresponding volume, t is the time, and x is the space coordinate (defined to be in the center of the volume element). Since we shall be considering only stationary solutions, the t dependence of the current will be omitted in the following sections. We also mention here, that we average (19) and (20) over many events in order to reduce statistical fluctuations.

Using Eqs. (19) and (20) we can determine all necessary macroscopic quantities. Then, using Eqs. (19) and (11), we compute the four-velocity in the Eckart frame and extract the particle number density, n , and the projection operator $\Delta^{\mu\nu}$. Finally, we compute the heat flow current using Eqs. (9) and (12).

V. ANALYTICAL EXPRESSION FOR THE GRADIENTS

In this work we aim to extract the gradient of a macroscopic quantity, such as the temperature T or the particle density n . The gradients are usually computed using finite-difference methods which demands a large amount of statistics in order to obtain a sufficiently smooth profile. Therefore, if one is able to obtain the general form of the solution that such gradients must satisfy in the stationary regime, it would save a huge amount of computational runtime.

As already shown in [38], quantities that are conserved in collisions show a linear behavior between the thermal reservoirs. For the boundary conditions implemented in this work, this is realized for the particle density.

For the type of boundary condition considered in this work, the particle number density satisfies the following solution in the stationary regime

$$n(x) = \frac{n_R^{\text{res}} - n_L^{\text{res}}}{L + 2\lambda_{\text{mfp}}} x + \frac{n_R^{\text{res}} + n_L^{\text{res}}}{2}, \quad (21)$$

where n_L^{res} and n_R^{res} are the particle number density in the left and right reservoirs, respectively, and L is the size of the static box in the x direction. We remark that this solution might be modified when inelastic collisions are included.

In general, the above solution does not hold near the boundaries (in the x -direction) of the static box, where the particle number density is discontinuous (see Ref. [38] for details). If the mean free-path, λ_{mfp} , of the particles is large compared to the size of the box, L , such discontinuity will lead to deviations from the above solution. Here we tackle this problem by making sure that $L \gg \lambda_{\text{mfp}}$. This will reduce such finite-size effects to the minimum amount possible and guarantees that the solution in Eq. (21) provides a very good description of the particle number density in most parts of the system. Using Eq. (21) and the fact that the thermodynamic pressure is constant inside the box, it is straightforward to obtain the temperature profile,

$$T(x) = p \left(\frac{n_R^{\text{res}} - n_L^{\text{res}}}{L + 2\lambda_{\text{mfp}}} x + \frac{n_R^{\text{res}} + n_L^{\text{res}}}{2} \right)^{-1}. \quad (22)$$

In Fig. 2, we show the particle number density (a), thermodynamic pressure (b), and temperature (c) profiles computed with BAMPS (dots) at $t = 50$ fm/c and $\sigma_{22} = 10$ mb, with the boundary conditions specified in the previous section. The blue curves correspond to

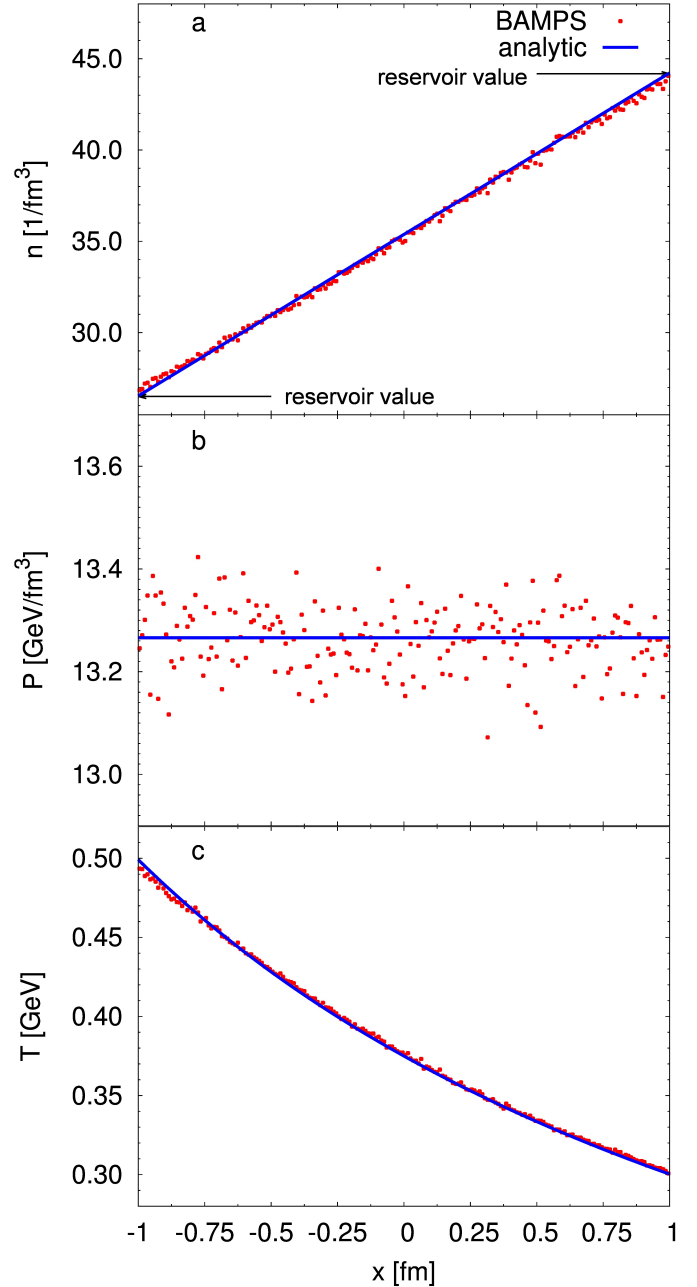


Figure 2. The numerical solutions extracted from BAMPS for particle density n , pressure P and temperature T . The cross section is set to $\sigma_{22} = 10$ mb. The solutions are shown at very late times, $t = 50$ fm/c, where the profiles are almost static. The reservoir values are chosen on the left (right) to $T_L^{\text{res}} = 0.5$ GeV and $\lambda_L^{\text{res}} = 1.0$ ($T_R^{\text{res}} = 0.3$ GeV and $\lambda_R^{\text{res}} = 7.72$). We compare each profile with the analytical results derived from Eq. (21). The results are averaged over 500 events.

the analytical solution described above. It is clear that Eq. (21) does in fact reproduce the solutions obtained numerically with BAMPS and that finite-size effects are negligible. Also, we confirm that the thermodynamic

pressure is constant, as it should be.

VI. EXTRACTION OF THE HEAT CONDUCTIVITY

Since the gradients of the particle number density and temperature can be computed analytically from Eqs. (21) and (22), and the pressure p is by construction constant, the extraction of the heat conductivity from BAMPs simulations becomes straightforward. Using $n(x) \equiv ax + b$ for the particle density and the relation (13) we can simplify Eq. (17) to

$$q^x = \kappa p \frac{a}{(ax + b)^2}. \quad (23)$$

Finally, the heat conductivity can be calculated using

$$\kappa = q^x \cdot \frac{(ax + b)^2}{ap}, \quad (24)$$

where the heat flow q^x is directly extracted from BAMPs and the constants a and b as well as the constant pressure p are analytically known.

Figure 3 shows the heat conductivity as function of x , at $t = 5$ fm. We use for the cross section $\sigma_{22} = 43$ mb. It is clear that κ is constant over space, which confirms that we reached the asymptotic solution. In Fig. 4 we show the heat conductivity as function of time t . The system relaxes locally on a very short time scale to its stationary solution, and the heat conductivity is afterwards basically constant over time. We remark, that the relaxation time is proportional to the mean free path, λ_{mfp} (see Ref. [35]).

In order to extract a precise value for heat conductivity κ , we take an average over the values obtained in the whole system and at all time steps that had reached the asymptotic state.

VII. RESULTS

In kinetic theory, there are several different methods to compute the transport coefficients appearing in the fluid-dynamical equations of motion, e.g. Chapman-Enskog theory and the many variations of the method of moments. The problem is that each method predicts different expressions for the transport coefficients. Even though these differences are not so large for the shear viscosity coefficient, which has been discussed in details in Refs. [37, 38], they can be significantly large for heat conductivity, as will be discussed in the following. The results from BAMPs can help to clarify which method reflects more reliably the underlying microscopic theory.

The method of moments, initially developed by H. Grad for nonrelativistic systems [45] and further extended to describe relativistic systems by several authors, is one of the most commonly employed methods

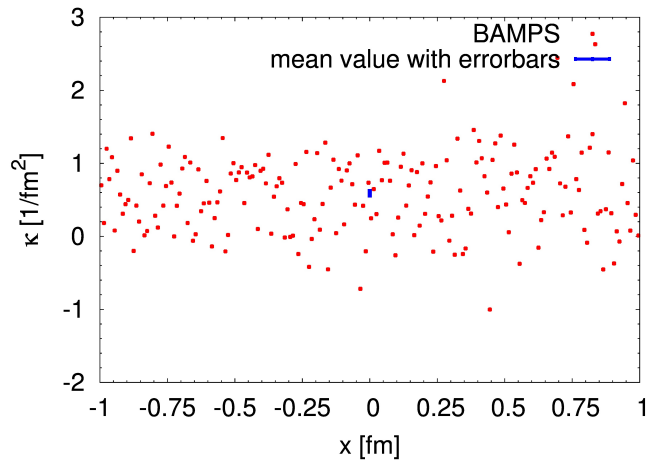


Figure 3. Heat conductivity coefficient extracted from BAMPs shown at every point in space. The mean value with error bar is also displayed. The results are shown at $t = 5$ fm/c for $\sigma_{22} = 43$ mb. 500 events were averaged.

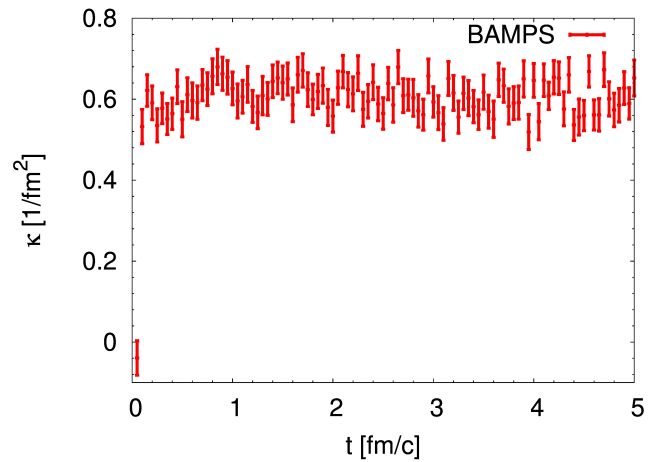


Figure 4. Heat conductivity coefficient extracted from BAMPs shown at different times averaged over the all positions in space. The results are shown for $\sigma_{22} = 43$ mb. 500 events were averaged.

in heavy ion collisions. Traditionally, this method is employed in the relativistic regime together with the so-called 14-moment approximation, originally proposed by Israel and Stewart [34]. In this scheme, the momentum distribution function, $f(x, p)$, is expanded in momentum space around its local equilibrium value in terms of a series of Lorentz tensors formed of particle four-momentum k^μ , i.e., $1, k^\mu, k^\mu k^\nu, \dots$. The 14-moment approximation consists in truncating the expansion at second order in momentum, i.e., keeping only the tensors $1, k^\mu$, and $k^\mu k^\nu$ in the expansion, leaving 14 unknown expansion coefficients. The coefficients of the truncated expansion are then uniquely matched to the 14 components of N^μ and $T^{\mu\nu}$.

Israel and Stewart obtained the equations of motion

of fluid dynamics and, consequently, the microscopic expressions of the transport coefficients appearing in such equations, by substituting the momentum distribution function truncated according to the 14-moment approximation into the second moment of the Boltzmann equation,

$$\int \frac{d^3k}{k^0} k^\mu k^\nu k^\lambda \partial_\mu f = \int \frac{d^3k}{k^0} k^\nu k^\lambda C[f].$$

By projecting this equation with $\Delta_\nu^\alpha u_\lambda$, Israel and Stewart obtained an equation of motion for the heat flow and a microscopic formula for κ [34, 46]. For a massless and classical gas of hard spheres, one obtains the following expression for the heat conductivity [36, 46],

$$\kappa = \frac{2}{\sigma_{22}}. \quad (25)$$

Note that Israel-Stewart's 14-moment approximation leads to ambiguous results since it can be substituted in any moment of the Boltzmann equation [46]. By changing the moment in which the 14-moment approximation is replaced, the equations of motion remain with the same general form, but the transport coefficients become different. For example, using the choice of moment applied in Ref. [47], one obtains a quantitatively different result for κ ,

$$\kappa = \frac{3}{\sigma_{22}}. \quad (26)$$

Naturally, other choices of moment will lead to even more different results, but we shall not list them all here.

Recently, the derivation of fluid dynamics from the method of moments was extended in order to remove the ambiguities of the 14-moment approximation [35]. The main difference between the 14-moment approximation and the theory derived in Ref. [35], namely Resummed Transient Relativistic Fluid Dynamics (RTRFD), is that the latter does not truncate the moment expansion of the momentum distribution function. Instead, dynamical equations for all its moments are considered and solved by separating the slowest microscopic time scale from the faster ones. The resulting fluid-dynamical equations are truncated according to a systematic power-counting scheme using the inverse Reynolds and the Knudsen numbers. The values of the transport coefficients of fluid dynamics are obtained by re-summing the contributions from all moments of the momentum distribution function, similar to what happens in Chapman-Enskog theory [48]. In practice, the transport coefficients are given by a summation of terms, each term originating from a specific moment of $f(x, p)$. Once the transport coefficients have converged, the summation can be truncated and the moments that are irrelevant can be dropped out. For the case of a massless and classical gas of hard spheres, the first three moments are enough to obtain a convergent value for κ , and one obtains [35]

$$\kappa = \frac{2.5536}{\sigma_{22}}. \quad (27)$$

Including the next moment would only lead to $\sim 1\%$ corrections to this expression.

Finally, heat conductivity can also be computed using Chapman-Enskog theory, as was done in Ref. [36] for a gas of classical and massless hard spheres,

$$\kappa = \frac{2.44}{\sigma_{22}}. \quad (28)$$

Note that the convergence of the above value was not investigated in Ref. [36] and, consequently, it is not possible to infer how precise this result is.

We found excellent agreement to the result of Ref. [35], i.e., Eq.(27). This can be seen in Fig. 5, where re-

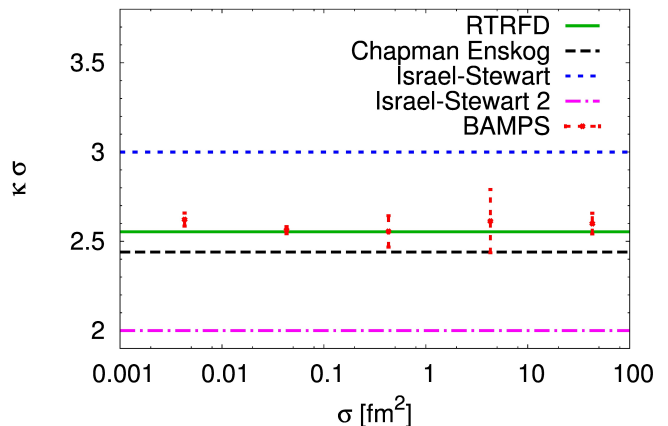


Figure 5. The dimensionless quantity $\kappa\sigma$ derived from different fluid dynamical theories (lines) compared to the results extracted directly from BAMPS (dots).

sults obtained using BAMPS are compared to Eqs. (25), (26), (27) and (28). The original Israel-Stewart theory (25) yields values roughly $\sim 22\%$ too low, while the 14-moment approximation with the choice of moment described in Ref. [47] leads to a result that is $\sim 17\%$ too high. The transport coefficient computed via Chapman-Enskog theory is close to the value obtained from microscopic theory, being $\sim 4\%$ below it. However, it is not clear whether this can be considered as a failure of the Chapman-Enskog theory since the precision of that result was not clearly stated and it may be possible that it can be improved to match what was extracted from the Boltzmann equation. Finally, the heat conductivity coefficient computed in Ref. [35] was basically the same as the one computed by BAMPS, within the errors of both the theoretical calculation (originating from the truncation of the moment expansion in the expression for κ) and the numerical one (originating from the finite statistics of the calculation). Nevertheless, all theoretical calculations predicted a $1/\sigma_{22}$ dependence of the heat conductivity coefficient on the cross section; a fact also confirmed by BAMPS, see Tab. I and Fig. 5.

σ_{22}	$\kappa [1/fm^2]$
0.043 mb	609.695698 ± 8.4513
0.43 mb	59.588731 ± 0.4694
4.3 mb	5.943535 ± 0.2041
43 mb	0.607672 ± 0.0411
430 mb	0.060449 ± 0.0013

Table I. Numerical results for the heat conductivity coefficient κ for various elastic cross sections over several orders of magnitude.

VIII. CONCLUSION AND OUTLOOK

In this work we extracted the heat conductivity coefficient for a dilute gas of massless and classical particles described by the relativistic Boltzmann equation. For this purpose we employed the microscopic transport model BAMPS in a static system using only binary collisions and a constant isotropic cross section. For this setup, we established a stationary temperature gradient using thermal reservoirs. In order to simplify the calculations we derived an analytical expression of the expected profile to obtain the gradients of the temperature, meanwhile the heat flow was extracted directly from BAMPS by the general decomposition of the particle four-flow and energy momentum tensor. Using the relativistic Navier-Stokes theory, which is valid for a stationary system and small gradients, we extracted the heat conductivity to a very high precision. We then compared this result with several theoretical predictions for this transport coefficient, each originating from a different derivation of fluid dynamics from the underlying microscopic theory.

The numerical simulations of the Boltzmann equation, realized in this paper with BAMPS, were able to distinguish between all these different theoretical results and clearly point out which one was in better agreement with the underlying microscopic theory. While Israel-Stewart

theory, i.e., the 14-moment approximation, performed rather poorly in the description of heat flow, new extensions of the method of moments, i.e. RTRFD, were able to provide an improved description of this transport coefficient, showing a very good agreement with the coefficient extracted from BAMPS. The heat conductivity computed using Chapman-Enskog theory was not able to precisely describe the simulation from BAMPS, although it was not as far off as the predictions using the 14-moment approximation. Nevertheless, this disagreement might be originating from a poor implementation of the Chapman-Enskog theory, which was not properly checked for the convergence of the transport coefficient.

The extracted value for the heat conductivity

$$\kappa_{\text{BAMPS}} = \frac{2.59 \pm 0.07}{\sigma_{22}}. \quad (29)$$

can be referred to as a literature value, within the numerical uncertainties, for the simple case of binary collisions with an isotropic cross section. It remains as a future task to extend this work to include inelastic scatterings, where particle production and annihilation have to be taken into account.

IX. ACKNOWLEDGMENTS

The authors are grateful to the Center for the Scientific Computing (CSC) at Frankfurt for the computing resources. FR and IB are grateful to “Helmholtz Graduate School for Heavy Ion research”. FR and ZX acknowledges supported by BMBF. GSD is supported by the Natural Sciences and Engineering Research Council of Canada. ZX is supported by the NSFC under grant No. 11275103. This work was supported by the Helmholtz International Center for FAIR within the framework of the LOEWE program launched by the State of Hesse.

-
- [1] D. H. Rischke, “The Quark gluon plasma in equilibrium,” *Prog.Part.Nucl.Phys.*, vol. 52, pp. 197–296, 2004.
 - [2] M. Tannenbaum, “Recent results in relativistic heavy ion collisions: From ‘a new state of matter’ to ‘the perfect fluid’,” *Rept.Prog.Phys.*, vol. 69, pp. 2005–2060, 2006.
 - [3] P. F. Kolb and U. W. Heinz, “Hydrodynamic description of ultrarelativistic heavy ion collisions,” 2003.
 - [4] I. Arsene *et al.*, “Quark gluon plasma and color glass condensate at RHIC? The Perspective from the BRAHMS experiment,” *Nucl.Phys.*, vol. A757, pp. 1–27, 2005.
 - [5] J. Adams *et al.*, “Experimental and theoretical challenges in the search for the quark gluon plasma: The STAR Collaboration’s critical assessment of the evidence from RHIC collisions,” *Nucl.Phys.*, vol. A757, pp. 102–183, 2005.
 - [6] K. Adcox *et al.*, “Formation of dense partonic matter in relativistic nucleus-nucleus collisions at RHIC: Experimental evaluation by the PHENIX collaboration,” *Nucl.Phys.*, vol. A757, pp. 184–283, 2005.
 - [7] B. Back, M. Baker, M. Ballintijn, D. Barton, B. Becker, *et al.*, “The PHOBOS perspective on discoveries at RHIC,” *Nucl.Phys.*, vol. A757, pp. 28–101, 2005.
 - [8] U. W. Heinz, H. Song, and A. K. Chaudhuri, “Dissipative hydrodynamics for viscous relativistic fluids,” *Phys.Rev.*, vol. C73, p. 034904, 2006.
 - [9] P. Romatschke and U. Romatschke, “Viscosity Information from Relativistic Nuclear Collisions: How Perfect is the Fluid Observed at RHIC?,” *Phys.Rev.Lett.*, vol. 99, p. 172301, 2007.
 - [10] M. Luzum and P. Romatschke, “Conformal Relativistic Viscous Hydrodynamics: Applications to RHIC results at $s(\text{NN})^{1/2} = 200\text{-GeV}$,” *Phys.Rev.*, vol. C78, p. 034915, 2008.

- [11] M. Luzum and J.-Y. Ollitrault, “Extracting the shear viscosity of the quark-gluon plasma from flow in ultra-central heavy-ion collisions,” 2012.
- [12] H. Song, S. A. Bass, and U. Heinz, “Viscous QCD matter in a hybrid hydrodynamic+Boltzmann approach,” *Phys.Rev.*, vol. C83, p. 024912, 2011.
- [13] H. Song, S. A. Bass, U. Heinz, T. Hirano, and C. Shen, “200 A GeV Au+Au collisions serve a nearly perfect quark-gluon liquid,” *Phys.Rev.Lett.*, vol. 106, p. 192301, 2011.
- [14] H. Song, S. A. Bass, and U. Heinz, “Elliptic flow in 200 A GeV Au+Au collisions and 2.76 A TeV Pb+Pb collisions: insights from viscous hydrodynamics + hadron cascade hybrid model,” *Phys.Rev.*, vol. C83, p. 054912, 2011.
- [15] H. Song, S. A. Bass, U. Heinz, T. Hirano, and C. Shen, “Hadron spectra and elliptic flow for 200 A GeV Au+Au collisions from viscous hydrodynamics coupled to a Boltzmann cascade,” *Phys.Rev.*, vol. C83, p. 054910, 2011.
- [16] B. Schenke, S. Jeon, and C. Gale, “Elliptic and triangular flow in event-by-event (3+1)D viscous hydrodynamics,” *Phys.Rev.Lett.*, vol. 106, p. 042301, 2011.
- [17] B. Schenke, S. Jeon, and C. Gale, “Anisotropic flow in $\sqrt{s} = 2.76$ TeV Pb+Pb collisions at the LHC,” *Phys.Lett.*, vol. B702, pp. 59–63, 2011.
- [18] B. Schenke, “Flow in heavy-ion collisions - Theory Perspective,” *J.Phys.*, vol. G38, p. 124009, 2011.
- [19] H. Niemi, G. S. Denicol, P. Huovinen, E. Molnar, and D. H. Rischke, “Influence of the shear viscosity of the quark-gluon plasma on elliptic flow in ultrarelativistic heavy-ion collisions,” *Phys.Rev.Lett.*, vol. 106, p. 212302, 2011.
- [20] H. Niemi, G. Denicol, P. Huovinen, E. Molnar, and D. Rischke, “Influence of a temperature-dependent shear viscosity on the azimuthal asymmetries of transverse momentum spectra in ultrarelativistic heavy-ion collisions,” *Phys.Rev.*, vol. C86, p. 014909, 2012.
- [21] V. Roy and A. Chaudhuri, “Charged particle’s elliptic flow in 2+1D viscous hydrodynamics at LHC ($\sqrt{s}= 2.76$ TeV) energy in Pb+Pb collision,” *Phys.Lett.*, vol. B703, pp. 313–317, 2011.
- [22] G. Denicol, T. Kodama, T. Koide, and P. Mota, “Effect of bulk viscosity on Elliptic Flow near QCD phase transition,” *Phys.Rev.*, vol. C80, p. 064901, 2009.
- [23] G. Denicol, T. Kodama, T. Koide, and P. Mota, “Bulk viscosity effects on elliptic flow,” *Nucl.Phys.*, vol. A830, pp. 729C–732C, 2009.
- [24] G. Denicol, T. Kodama, and T. Koide, “The effect of shear and bulk viscosities on elliptic flow,” *J.Phys.*, vol. G37, p. 094040, 2010.
- [25] A. Monnai and T. Hirano, “Effects of Bulk Viscosity at Freezeout,” *Phys.Rev.*, vol. C80, p. 054906, 2009.
- [26] A. Monnai and T. Hirano, “Effects of Bulk Viscosity on p(T)-Spectra and Elliptic Flow Parameter,” *Nucl.Phys.*, vol. A830, pp. 471C–474C, 2009.
- [27] T. Schaefer and K. Dusling, “Bulk viscosity, chemical equilibration and flow at RHIC,” 2012.
- [28] K. Dusling and T. Schaefer, “Bulk viscosity, particle spectra and flow in heavy-ion collisions,” *Phys.Rev.*, vol. C85, p. 044909, 2012.
- [29] P. Bozek, “Bulk and shear viscosities of matter created in relativistic heavy-ion collisions,” *Phys.Rev.*, vol. C81, p. 034909, 2010.
- [30] V. Roy and A. Chaudhuri, “2+1 dimensional hydrodynamics including bulk viscosity: A Systematics study,” *Phys.Rev.*, vol. C85, p. 024909, 2012.
- [31] V. Roy and A. Chaudhuri, “Bulk viscosity in heavy ion collision,” 2012.
- [32] H. Song and U. W. Heinz, “Interplay of shear and bulk viscosity in generating flow in heavy-ion collisions,” *Phys.Rev.*, vol. C81, p. 024905, 2010.
- [33] G. Denicol, H. Niemi, I. Bouras, E. Molnar, Z. Xu, *et al.*, “Solving the heat-flow problem with transient relativistic fluid dynamics,” 2012.
- [34] W. Israel and J. Stewart, “Transient relativistic thermodynamics and kinetic theory,” *Annals Phys.*, vol. 118, pp. 341–372, 1979.
- [35] G. Denicol, H. Niemi, E. Molnar, and D. Rischke, “Derivation of transient relativistic fluid dynamics from the Boltzmann equation,” *Phys.Rev.*, vol. D85, p. 114047, 2012.
- [36] S. Groot, W. van Leeuwen, and van Weert Ch.G., *Relativistic Kinetic Theory*. Elsevier North-Holland, INC. 52 Vanderbilt Avenue, New York, N.Y. 10017: North-Holland Publishing Company, 1980.
- [37] C. Wesp, A. El, F. Reining, Z. Xu, I. Bouras, *et al.*, “Calculation of shear viscosity using Green-Kubo relations within a parton cascade,” *Phys.Rev.*, vol. C84, p. 054911, 2011.
- [38] F. Reining, I. Bouras, A. El, C. Wesp, Z. Xu, *et al.*, “Extraction of shear viscosity in stationary states of relativistic particle systems,” *Phys.Rev.*, vol. E85, p. 026302, 2012.
- [39] Z. Xu and C. Greiner, “Thermalization of gluons in ultra-relativistic heavy ion collisions by including three-body interactions in a parton cascade,” *Phys.Rev.*, vol. C71, p. 064901, 2005.
- [40] C. Eckart, “The Thermodynamics of irreversible processes. 3.. Relativistic theory of the simple fluid,” *Phys.Rev.*, vol. 58, pp. 919–924, 1940.
- [41] I. Bouras, E. Molnar, H. Niemi, Z. Xu, A. El, *et al.*, “Relativistic shock waves in viscous gluon matter,” *Phys.Rev.Lett.*, vol. 103, p. 032301, 2009.
- [42] I. Bouras, E. Molnar, H. Niemi, Z. Xu, A. El, *et al.*, “Investigation of shock waves in the relativistic Riemann problem: A Comparison of viscous fluid dynamics to kinetic theory,” *Phys.Rev.*, vol. C82, p. 024910, 2010.
- [43] O. Fochler, “Investigation of high-pt phenomena within a partonic transport model.” PHD thesis, 2011.
- [44] J. Uphoff, O. Fochler, Z. Xu, and C. Greiner, “Elliptic Flow and Energy Loss of Heavy Quarks in Ultra-Relativistic heavy Ion Collisions,” *Phys.Rev.*, vol. C84, p. 024908, 2011.
- [45] H. Grad., “On the kinetic theory of rarefied gases,” *Comm. Pure Appl. Math*, vol. 2, pp. 331–407, 1949.
- [46] G. Denicol, E. Molnar, H. Niemi, and D. Rischke, “Derivation of fluid dynamics from kinetic theory with the 14-moment approximation,” 2012.
- [47] G. Denicol, T. Koide, and D. Rischke, “Dissipative relativistic fluid dynamics: a new way to derive the equations of motion from kinetic theory,” *Phys.Rev.Lett.*, vol. 105, p. 162501, 2010.
- [48] S. Chapman and T. Cowling, *The mathematical theory of non-uniform gases*. Cambridge: Cambridge University Press, 3rd edition ed., 1991.